# Quasiparticle tunneling current-voltage characteristics of intrinsic Josephson junctions in $Bi_2Sr_2CaCu_2O_{8+\delta}$

Michihide Kitamura, Akinobu Irie, and Gin-ichiro Oya
*Department of Electrical and Electronic Engineering, Utsunomiya University, 7-1-2 Yoto, Utsunomiya, Tochigi 321-8585, Japan*
(Received 4 February 2002; published 14 August 2002)

A model to understand the overall profile of the quasiparticle (QP) tunneling current-voltage ($I$-$V$) characteristic of intrinsic Josephson junctions in high-$T_c$ superconductors such as $Bi_2Sr_2CaCu_2O_{8+\delta}$ is presented. It is mentioned that the angular dependence of the energy gap $\Delta_{\mathbf{k}}$ should be represented to be of $\sin^{2n}\theta\cos 2\phi$ type rather than the $\theta$-independent purely two dimensional $\cos 2\phi$ one. It is shown that the QP $I$-$V$ characteristic calculated on the basis of our model including no empirical parameters well predicts our experimental $I$-$V$ characteristic, and that the QP $I$-$V$ characteristic calculated using $n=2$ is in very good agreement with the experiment on the whole voltage region.

DOI: 10.1103/PhysRevB.66.054519 PACS number(s): 74.25.Fy, 74.25.Jb, 74.50.+r, 74.72.Hs

## I. INTRODUCTION

Since the discovery of superconductivity at ~35 K in $La_{2-x}Ba_xCuO_4$ (LBCO) by Bednorz and Müller[1] in 1986, the study of superconductivity has greatly developed in order to search for superconducting materials with high-transition temperatures: so-called ''high-$T_c$ superconductors.'' Actually, Wu *et al.*[2] found $YBa_2Cu_3O_{7-\delta}$ (YBCO) with $T_c\sim 90$ K in 1987, Maeda *et al.*[3] discovered $Bi_2Sr_2CaCu_2O_{8+\delta}$ (BSCCO) with $T_c\sim 90$ K in 1988, in the same year Sheng and Hermann[4] also found $Tl_2Ba_2Ca_2Cu_3O_{10+\delta}$ (TBCCO) with $T_c\sim 130$ K, and recently $HgBa_2Ca_2CuO_8$ with $T_c=134$ K was discovered by Schilling *et al.*[5] The common properties observed on these high-$T_c$ superconductors are that all the materials have superconducting layers (SL's) consisting of $CuO_2$ planes, and superconductors such as BSCCO in particular have an inherent structure consisting of alternate stacks of (SL's) and insulating layer (IL's) along the $c$ axis, and hence they present anisotropic characteristics in directions parallel and perpendicular to the $c$ axis. A stack of SL's and IL's, which is formed *naturally*, makes a series array of superconductor-insulator-superconductor (SIS) junctions. The SIS junction works well as a Josephson junction when a weak interaction is established between the superconducting wave functions of the two SL's. Therefore, it is expected that the high-$T_c$ superconductor becomes a good candidate for the Josephson device which operates in high-temperature region (>77 K).

From experiments for the transport properties of layered high-$T_c$ superconductors along the $c$ axis, it was found that BSCCO, Pb-substituted BSCCO, TBCCO, and underdoped YBCO make intrinsic Josephson junction (IJJ) structure.[6–15] The $I$-$V$ characteristic of superconductors constructed many of SIS junctions such as BSCCO can be summarized as follows if the nonequilibrium effect is not taken into account: (1) As an external bias current $I_{ext}$ increases, a tunneling current $I_T$ increases up to a critical current $I_C$ without an occurrence of a voltage difference due to Cooper pairs (CP's) tunneling (the dc Josephson effect). This process is reversible, i.e., $I_T$ decreases with decreasing $I_{ext}$ and reaches zero. This $I$-$V$ line does not originate from quasiparticles (QP's), and the CP tunneling is called the zeroth branch. (2) When $I_T$ reaches $I_C$, if all the $N$ SIS junctions have ideally the same characteristics, a voltage jump of $V$ occurs at the same time over all the $N$ junctions, and hence a net voltage jump of $NV$ occurs on the $I$-$V$ characteristics. Actually, however, the $I$-$V$ characteristics of a SIS junction somewhat differ from those of the others because of their crystal incompleteness and dimension irregularity, so that usually a voltage jump of $V$ for the junction with the lowest $I_C$ occurs on the $I$-$V$ characteristics. In the voltage state on the $I$-$V$ curve (not a line), the $I_T$ rapidly decreases with decreasing voltage difference, and finally reaches zero. This curve as the first branch originates from QP tunneling with an accompanying ac Josephson oscillation. (3) The $I$-$V$ characteristics of superconductors constructed from $N$-SIS junctions exihibit $N$ branches with hysteresis. If we focus the $n$th branch ($1\leqslant n<N$), the net voltage jump of $nV$ is observed when $I_T=I_C$ for the $n$th junction, and the $I$-$V$ characteristic of the $n$th branch shows a behavior similar to that of the first one, i.e., $I_T$ rapidly decreases with decreasing the $I_{ext}$. (4) On the $N$th branch in which all the junctions are in the voltage state, both the QP tunneling current and the ac Josephson current flow across the junctions. It is well known that on the intrinsic Josephson junctions (IJJ's) of BSCCO, the current observed at the voltage $NV$, $I_{NV}$, is about 20 times larger than that observed at the voltage $nV$, $I_{nV}(=I_T)$ where $1\leqslant n<N$.[15] In the present paper, we focus our attention to only the $I$-$V$ characterisic of $N$th branch, so that we do not consider why $I_{nV}$ is about 20 times smaller than $I_{NV}$.

In the present paper, we theoretically consider the QP tunneling $I$-$V$ characteristic of the $N$th branch along the $c$-axis observed experimentally for the high-$T_c$ superconductors having an IJJ structure such as BSCCO and TBCCO. In order to calculate the $N$th branch QP tunneling $I$-$V$ characteristic of SIS junctions, usually, the following equation is widely used [hereafter we call this the density of states, (DOS), model];[16,17]

$$I(V)=\text{const}\times\int_{-\infty}^{\infty}N(E)N(E-eV)\{f(E-eV)-f(E)\}dE, \tag{1}$$

 

where $f(E)$ is the Fermi-Dirac distribution function and $N(E)$ is the density of states of the QP in the superconductor. It should be noted here that in the DOS model the symmetry of the crystal is taken into account only in $N(E)$ since $E$ is an integral variable. If the energy gap $\Delta$ of the superconductor is independent of the wave number $\mathbf{k}$, i.e., the *s*-symmetry energy gap, it is not so bad to calculate the $I$-$V$ characteristic using the DOS model. However, it is well known that the energy gap of high-$T_c$ superconductors such as BSCCO and TBCCO has a $d_{x^2-y^2}$ symmetry rather than the *s* symmetry found in metal superconductors (low-$T_c$ superconductors).[18–23] Therefore, when the $I$-$V$ characteristic of a SIS junction constructed from superconductors with a $d_{x^2-y^2}$-symmetry energy gap is calculated using the DOS model, $N(E)$ must be represented so as to include the symmetry of the energy gap and the crystal. This is usually done by an averaging treatment;[12,14,24]

$$N(E)=\frac{1}{2\pi}\int_0^{2\pi} N_n(\phi)\frac{E}{\sqrt{E^2-\Delta(\phi)^2}}d\phi, \tag{2}$$

where $\phi$ is the angle defined in the polar coordinate, and the energy gap $\Delta(\phi)=\Delta_0\cos 2\phi$ and the density of states at Fermi level of normal state $N_n(\phi)$ in the superconductors are assumed to have only a $\phi$ dependence. Even if the $d_{x^2-y^2}$ symmetry $\cos 2\phi$-type energy gap and the density of states, calculated and measured as correctly as possible, are adopted for the $\Delta(\phi)$ and $N_n(\phi)$, the density of states $N(E)$ calculated using Eq. (2) is an averaged value so that this treatment is not so correct. Actually, Tanabe *et al.*,[12] Itoh *et al.*,[14] and Schlenga *et al.*[24] independently calculated the QP $I$-$V$ characteristics of BSCCO using the DOS model and found that it is possible to explain partly the QP $I$-$V$ characteristic of BSCCO but not so easy to explain fairly well the overall profile of the QP $I$-$V$ characteristic using the DOS model. The method to avoid this approximative treatment is to do the calculation by using the wave number $\mathbf{k}$ which characterizes the Cooper pair $(\mathbf{k}\sigma,-\mathbf{k}\sigma')$ instead of the integral by $E$. Here it is noted that we consider a CP with a singlet state so that the spin state $(\sigma,\sigma')$ is given by $(\uparrow,\downarrow)$ or $(\downarrow,\uparrow)$.

As far as we know, there is no model to explain the overall profile of the QP $I$-$V$ characteristic of BSCCO with no adjustable parameters. The aim of this paper is to present a model to explain the overall profile of the QP $I$-$V$ characteristics of BSCCO.

## II. THEORY

### A. Model

In this section, we formulate the QP tunneling $I$-$V$ characteristic of a SIS junction constructed by superconductors with a $d_{x^2-y^2}$ symmetry energy gap. In superconductors, QP's are generated by the separation of *a* CP $(\mathbf{k}\sigma,-\mathbf{k}\sigma')$, so that a CP makes two QP's, one $\mathbf{k}\sigma$ and the other $-\mathbf{k}\sigma'$. Here we assume that the electronic states in the vicinity of the Fermi level $E_F$ show no electron spin dependence, i.e., there is no magnetic order. If so, the existing probabilities of electrons with spin-up and spin-down states become indentical to each other. We consider electronic states with no magnetic order, so that the model deduced in the present paper is applicable to superconductors whose electronic structures show no electron spin dependence.

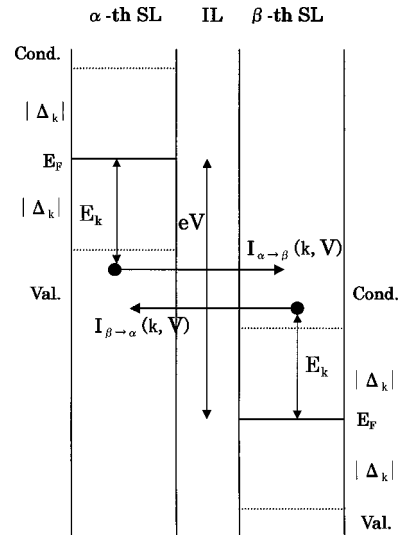


FIG. 1. Interpretation based on the semiconductor model for the tunneling process of the quasiparticle (QP) specified by the wave number $\mathbf{k}$. The $\alpha$th and $\beta$th superconducting layers (SL's) with the energy difference $eV$ are separated by an insulating layer (IL). The tunneling of the QP having the wave number $\mathbf{k}$ occurs when the condition $eV \geqslant 2|\Delta_{\mathbf{k}}|$ is satisfied. The absolute value $|\Delta_{\mathbf{k}}|$ of the energy gap $\Delta_{\mathbf{k}}$ is a function of the $\mathbf{k}$ and ranges from 0 to the maximum value $\Delta_{max}$ defined as $eV_g/2$ using the threshold voltage $V_g$ observed experimentally. Therefore, it should be emphasized that the QP tunneling occurs even in the case of $V<V_g$, because the QP having the $\mathbf{k}$ which satisfies the condition $eV \geqslant 2|\Delta_{\mathbf{k}}|$ always exists.

Let us consider the tunneling current $I_{\alpha\to\beta}(\mathbf{k},V)$ of the QP specified by the wave number $\mathbf{k}$ from the $\alpha$th SL to the $\beta$th one on the basis of a semiconductor model shown in Fig. 1. This tunneling occurs when (1) the CP characterized by the wave number $\mathbf{k}$ exists, i.e., $v_{\mathbf{k}}^* v_{\mathbf{k}}=\frac{1}{2}[1-(\xi_{\mathbf{k}}/E_{\mathbf{k}})]\neq 0$, where $\xi_{\mathbf{k}}$ is the electron energy relative to the Fermi level $E_F$, $\varepsilon_{\mathbf{k}}-E_F$ and $E_{\mathbf{k}}$ is the excitation energy of the QP given by $\sqrt{\xi_{\mathbf{k}}^2+\Delta_{\mathbf{k}}^2}$; (2) the QP exists on the level identified by the energy $-E_{\mathbf{k}}$ in the valence band ($\xi_{\mathbf{k}}\leqslant 0$) of the $\alpha$th SL, i.e., $f(-E_{\mathbf{k}})\neq 0$; (3) the level identified by the energy $eV-E_{\mathbf{k}}$ ($\equiv\lambda_{\mathbf{k}}$) in the conduction band ($\xi_{\mathbf{k}}\geqslant 0$) of the $\beta$th SL is vacant, i.e., $\{1-f(\lambda_{\mathbf{k}})\}\neq 0$; and (4) the energy $\lambda_{\mathbf{k}}$ is larger than the absolute value of the energy gap, $|\Delta_{\mathbf{k}}|$. The transition probability $P_{\alpha\to\beta}(\mathbf{k})$ of the QP having a wave number $\mathbf{k}$ from the valence band of the $\alpha$th SL to the conduction band of the $\beta$th SL is given by

$$P_{\alpha\to\beta}(\mathbf{k})=\frac{2\pi}{\hbar}|T|^2 N_\beta^{(c)}(\lambda_{\mathbf{k}})\equiv\tau N_\beta^{(c)}(\lambda_{\mathbf{k}}), \tag{3}$$

assuming a $\mathbf{k}$-independent tunneling matrix element $T$, so that if we denote the charge of the QP to be transferred as

$q_{\mathbf{k}}$, the QP tunneling current $I_{\alpha\to\beta}(V)$ from the $\alpha$th SL to the $\beta$th SL (we define the direction $\alpha\to\beta$ as the $+z$ direction.) is given as

$$I_{\alpha\to\beta}(V)=\sum_{\mathbf{k}(k_z>0,\xi_{\mathbf{k}}\leqslant 0)} I_{\alpha\to\beta}(\mathbf{k},V)$$

$$=\tau\sum_{\mathbf{k}(k_z>0,\xi_{\mathbf{k}}\leqslant 0)} v_{\mathbf{k}}^{*}v_{\mathbf{k}}f(-E_{\mathbf{k}})q_{\mathbf{k}}\{1-f(\lambda_{\mathbf{k}})\}$$

$$\times N_{\beta}^{(c)}(\lambda_{\mathbf{k}})\Theta(\lambda_{\mathbf{k}}-|\Delta_{\mathbf{k}}|), \tag{4}$$

where $\Theta(x)$ is a step function defined as

$$\Theta(x)=\begin{cases}1(x\geqslant 0)\\ 0(x<0).\end{cases} \tag{5}$$

It is clear from Fig. 1 that the tunneling current $I_{\beta\to\alpha}(V)$ from the $\beta$th SL to the $\alpha$th SL is given by using the tunneling current $I_{\beta\to\alpha}(\mathbf{k},V)$, which is the current when the QP with the energy of $E_{\mathbf{k}}$ in the conduction band of the $\beta$th SL transfers to the valence band of the $\alpha$th SL with the energy of $E_{\mathbf{k}}-eV(=-\lambda_{\mathbf{k}})$, as follows:

$$I_{\beta\to\alpha}(V)=\sum_{\mathbf{k}(k_z<0,\xi_{\mathbf{k}}\geqslant 0)} I_{\beta\to\alpha}(\mathbf{k},V)$$

$$=\tau\sum_{\mathbf{k}(k_z<0,\xi_{\mathbf{k}}\geqslant 0)} v_{\mathbf{k}}^{*}v_{\mathbf{k}}f(E_{\mathbf{k}})q_{\mathbf{k}}\{1-f(-\lambda_{\mathbf{k}})\}$$

$$\times N_{\alpha}^{(v)}(-\lambda_{\mathbf{k}})\Theta(\lambda_{\mathbf{k}}-|\Delta_{\mathbf{k}}|). \tag{6}$$

Here we are considering a crystal with $D_{4h}$ symmetry, so it is noted that the $\Sigma_{\mathbf{k}(k_z<0)}$ is equal to $\Sigma_{\mathbf{k}(k_z>0)}$ because of the mirror symmetry on the horizontal plane. Symbols $v$ and $c$ labeled on the density of states are the characters introduced to represent the valence and conduction bands within the framework of the semiconductor model. Using the weight $v_{\mathbf{k}}^{*}v_{\mathbf{k}}$ for the energy $\lambda_{\mathbf{k}}$, which is the existing probability of the CP identified by the energy of $\lambda_{\mathbf{k}}$, given by

$$\frac{1}{2}\left(1-\frac{\sqrt{\lambda_{\mathbf{k}}^{2}-\Delta_{\mathbf{k}}^{2}}}{\lambda_{\mathbf{k}}}\right)\equiv w(\lambda_{\mathbf{k}},\Delta_{\mathbf{k}}), \tag{7}$$

and the density of states of the QP $N_{QP}(\lambda_{\mathbf{k}})$ given as

$$N_{QP}(\lambda_{\mathbf{k}})=\frac{N_n(E_F)|\lambda_{\mathbf{k}}|}{\sqrt{\lambda_{\mathbf{k}}^{2}-\Delta_{\mathbf{k}}^{2}}}, \tag{8}$$

the valence and the conduction bands can be represented as follows;

$$N_{\alpha}^{(v)}(-\lambda_{\mathbf{k}})=w(-\lambda_{\mathbf{k}},\Delta_{\mathbf{k}})N_{QP}(-\lambda_{\mathbf{k}}),$$

$$N_{\beta}^{(c)}(\lambda_{\mathbf{k}})=\{1-w(\lambda_{\mathbf{k}},\Delta_{\mathbf{k}})\}N_{QP}(\lambda_{\mathbf{k}}). \tag{9}$$

From Eq. (9), it is easily seen that

$$N_{\alpha}^{(v)}(-\lambda_{\mathbf{k}})=N_{\beta}^{(c)}(\lambda_{\mathbf{k}})=w(-\lambda_{\mathbf{k}},\Delta_{\mathbf{k}})N_{QP}(\lambda_{\mathbf{k}}), \tag{10}$$

so that we obtain the net tunneling current $I(V)$ for the QP $I$-$V$ characteristic as

$$I(V)=I_{\alpha\to\beta}(V)-I_{\beta\to\alpha}(V)$$

$$=\tau\sum_{\mathbf{k}(k_z>0,\xi_{\mathbf{k}}\leqslant 0)} v_{\mathbf{k}}^{*}v_{\mathbf{k}}q_{\mathbf{k}}w(-\lambda_{\mathbf{k}},\Delta_{\mathbf{k}})N_{QP}(\lambda_{\mathbf{k}})$$

$$\times\Theta(\lambda_{\mathbf{k}}-|\Delta_{\mathbf{k}}|)f(-E_{\mathbf{k}})\{1-f(\lambda_{\mathbf{k}})\}-\tau$$

$$\times\sum_{\mathbf{k}(k_z>0,\xi_{\mathbf{k}}\geqslant 0)} v_{\mathbf{k}}^{*}v_{\mathbf{k}}q_{\mathbf{k}}w(-\lambda_{\mathbf{k}},\Delta_{\mathbf{k}})N_{QP}(\lambda_{\mathbf{k}})$$

$$\times\Theta(\lambda_{\mathbf{k}}-|\Delta_{\mathbf{k}}|)f(E_{\mathbf{k}})\{1-f(-\lambda_{\mathbf{k}})\}, \tag{11}$$

where $\lambda_{\mathbf{k}}=eV-E_{\mathbf{k}}(\geqslant|\Delta_{\mathbf{k}}|\geqslant 0)$.

In Eq. (11), if we set $v_{\mathbf{k}}^{*}v_{\mathbf{k}}\to 1$, $q_{\mathbf{k}}\to q(\text{const})$ and $w(-\lambda_{\mathbf{k}},\Delta_{\mathbf{k}})\to 1$, we can see under the condition of $\lambda_{\mathbf{k}}\geqslant|\Delta_{\mathbf{k}}|$ that Eq. (11), our model reaches Eq. (1), the DOS model, as follows:

$$I(V)=q\tau\sum_{\mathbf{k}(k_z>0,\xi_{\mathbf{k}}\leqslant 0)} N_{QP}(\lambda_{\mathbf{k}})f(-E_{\mathbf{k}})\{1-f(\lambda_{\mathbf{k}})\}$$

$$-q\tau\sum_{\mathbf{k}(k_z>0,\xi_{\mathbf{k}}\geqslant 0)} N_{QP}(\lambda_{\mathbf{k}})f(E_{\mathbf{k}})\{1-f(-\lambda_{\mathbf{k}})\}. \tag{12}$$

Here if $\Sigma_{\mathbf{k}(k_z>0,\xi_{\mathbf{k}}\leqslant 0)}F(\mathbf{k})\simeq\frac{1}{2}\Sigma_{\mathbf{k}(k_z>0)}F(\mathbf{k})$ and $\Sigma_{\mathbf{k}(k_z>0,\xi_{\mathbf{k}}\geqslant 0)}F(\mathbf{k})\simeq\frac{1}{2}\Sigma_{\mathbf{k}(k_z>0)}F(\mathbf{k})$ are assumed for an arbitrary function $F(\mathbf{k})$, Eq. (12) is further evaluated as

$$I(V)=\frac{q\tau}{2}\sum_{\mathbf{k}(k_z>0)} N_{QP}(E_{\mathbf{k}}-eV)\{f(E_{\mathbf{k}}-eV)-f(E_{\mathbf{k}})\}$$

$$=\frac{q\tau}{4}\int_{-\infty}^{\infty}N_{QP}(E-eV)\{f(E-eV)-f(E)\}$$

$$\times\sum_{\mathbf{k}}\delta(E-E_{\mathbf{k}})dE$$

$$=\text{const}\int_{-\infty}^{\infty}N_{QP}(E)N_{QP}(E-eV)$$

$$\times\{f(E-eV)-f(E)\}dE. \tag{13}$$

This is just equal to Eq. (1).

Equation (11) tells us that the essential values on the calculation of the QP $I$-$V$ characteristic are $\Delta_{\mathbf{k}}$, $q_{\mathbf{k}}$, and $\xi_{\mathbf{k}}$. In the following we consider how these values are given or evaluated.

### B. Energy gap $\Delta_{\mathbf{k}}$

The energy gap $\Delta_{\mathbf{k}}$ satisfies a following self-consistent equation called "self-consistent gap equation"[25]

$$\Delta_{\mathbf{k}}=-\sum_{\mathbf{k}'}\frac{V_{\mathbf{k},\mathbf{k}'}}{2E_{\mathbf{k}'}}\Delta_{\mathbf{k}'}\tanh\frac{E_{\mathbf{k}'}}{2k_BT}. \tag{14}$$

Equation (14) tells us that the symmetry of the energy gap $\Delta_{\mathbf{k}}$ originates from that of $V_{\mathbf{k},\mathbf{k}'}$. Here $V_{\mathbf{k},\mathbf{k}'}$ is the matrix

element for the scattering of a CP from $(\mathbf{k}\sigma,-\mathbf{k}\sigma')$ to $(\mathbf{k}'\sigma,-\mathbf{k}'\sigma')$, and is defined by using a scattering potential $V(\mathbf{r})$ as

$$V_{\mathbf{k},\mathbf{k}'} \equiv \int e^{-i\mathbf{k}'\cdot\mathbf{r}} V(\mathbf{r}) e^{i\mathbf{k}\cdot\mathbf{r}} d\mathbf{r}. \tag{15}$$

In the following, therefore, we consider how the $V_{\mathbf{k},\mathbf{k}'}$ is evaluated for the high-$T_c$ superconductors such as the BSCCO.

CP's exist in a SL consisting of $CuO_2$ planes and the electronic states near the Fermi level are made from the $pd\sigma$-state constructed by the copper $3d_{x^2-y^2}$ and oxygen $2p_\sigma$ orbitals (which is clarified by the band-structure calculation carried out in the present paper). Therefore, it is sure that the scattering potential $V(\mathbf{r})$ has a site symmetry $D_{4h}$. If so, the potential $V(\mathbf{r})$ can be approximated as

$$V(\mathbf{r}) = \sum_l \sum_m v_{l,m}(r)\mathcal{Y}_l^m(\hat{\mathbf{r}}) \simeq v_{0,0}(r)\mathcal{Y}_0^0(\hat{\mathbf{r}}) + v_{4,4}(r)\mathcal{Y}_4^4(\hat{\mathbf{r}}), \tag{16}$$

where $\hat{\mathbf{r}}$ denotes the angular variables $\theta$ and $\phi$ of the vector $\mathbf{r}$, and $\mathcal{Y}_l^m(\hat{\mathbf{r}})$ is the spherical harmonics in a *real base*. $\mathcal{Y}_0^0(\hat{\mathbf{r}})$ is of course $\sqrt{(1/4\pi)}$ and $\mathcal{Y}_4^4(\hat{\mathbf{r}})$ is given by

$$\begin{aligned}\mathcal{Y}_4^4(\hat{\mathbf{r}}) &\equiv \sqrt{\frac{1}{2}}\{Y_4^4(\hat{\mathbf{r}}) + Y_4^{-4}(\hat{\mathbf{r}})\} \\ &= \left(\frac{3\sqrt{35}}{8\sqrt{4\pi}}\right)\left(\frac{x^4 - 6x^2y^2 + y^4}{r^4}\right),\end{aligned} \tag{17}$$

where $Y_l^m(\hat{\mathbf{r}})$ is the spherical harmonics in *complex base*. In low-$T_c$ superconductors, the most important part of the scattering potential is the spherical part $\sqrt{(1/4\pi)}v_{0,0}(r)$. This fact has made a foundation of the BCS theory in which the energy gap of the superconductor is given by the value with no-wavenumber dependence, i.e., an *s*-symmetry energy gap. As already stated, high-$T_C$ superconductors such as a BSCCO are, however, not bulk superconductors but superconductors with a series array of many SIS junctions constructed from thin superconducting layers (for example, the width of the SL is only about 3 Å in the case of BSCCO). Therefore, it is expected that the spherical part of the scattering potential is very small as compared with the nonspherical parts. It is easy to show that the nonspherical part $v_{4,4}(r)\mathcal{Y}_4^4(\hat{\mathbf{r}})$ makes a $\mathcal{Y}_2^2(\hat{\mathbf{k}})$ symmetry, i.e., $d_{x^2-y^2}$ symmetry, as the $\mathbf{k}$ dependence of the energy gap $\Delta_{\mathbf{k}}$. From the above, it could be sure that the energy gap $\Delta_{\mathbf{k}}$ can be represented as

$$\Delta_{\mathbf{k}} = \gamma(k)\mathcal{Y}_2^2(\hat{\mathbf{k}}). \tag{18}$$

As the energy gap having a $\mathcal{Y}_2^2(\hat{\mathbf{k}})$-type symmetry, the simplest $\cos 2\phi[=(x^2-y^2)/(x^2+y^2)\equiv\varphi(\phi)]$ type is usually adopted for the energy gap of the high-$T_c$ superconductors such as BSCCO. This is not wrong, but it should be noted that a function generated by the product of the function $\varphi(\phi)$ and the basis function $\varphi_{a_{1g}}(D_{4h})$ of the $a_{1g}$ irreducible representation of the group $D_{4h}$ also shows the same symmetry. There are some $\varphi_{a_{1g}}(D_{4h})$ basis functions such as 1, $z^2$, and $x^2+y^2$. Since the energy gap must not be permanently zero at $\theta=\pi/2$, i.e., $k_z=0$, in the present paper we adopt the $(x^2+y^2)^n$-type function as the basis function $\varphi_{a_{1g}}(D_{4h})$. That is, the energy gap $\Delta_{\mathbf{k}}$ used in the present paper is given as

$$\Delta_{\mathbf{k}} = \Delta(k,T)\sin^{2n}\theta\cos 2\phi \simeq \Delta(T)\sin^{2n}\theta\cos 2\phi, \tag{19}$$

where $n \geqslant 0$ and $\Delta(T)$ as a function of the temperature $T$ is the value of $\Delta(k,T)$ at the Fermi wave number $k=k_F$, and $\theta$ and $\phi$ are angles defined in the polar coordinate.

### C. Charge of quasiparticle $q_{\mathbf{k}}$

As already noted, QP's are generated by the separation of a CP. Hence it is reasonable to suppose that a QP holds the symmetry of the CP in $\mathbf{k}$ space. The $\mathbf{k}$-dependence of the charge of the CP is given by the square of the $\mathbf{k}$-dependent order parameter $\psi_{\mathbf{k}}$, and the symmetry of the order parameter is the same as that of the energy gap $\Delta_{\mathbf{k}}$. Therefore, the charge of the QP $q_{\mathbf{k}}$ should be proportional to the square of the energy gap, $|\Delta_{\mathbf{k}}|^2$, that is, $q_{\mathbf{k}}$ should be given as

$$q_{\mathbf{k}} = q\sin^{4n}\theta\cos^2 2\phi. \tag{20}$$

Equation (20) tells us that for a given $\theta$, i.e., for a given $k_z$, the the value of the QP charge which contributes to the tunneling current reaches a maximum when $\phi = n\pi/2$, and becomes zero when $\phi = (n \pm \frac{1}{4})\pi$. This is true because the existing probability of the CP reaches a maximum when the wave number $\mathbf{k}$ characterizing the CP satisfies the condition of $\phi = n\pi/2$, and becomes zero when $\mathbf{k}$ satisfies $\phi = (n \pm \frac{1}{4})\pi$.

### D. Value of $\xi_{\mathbf{k}}$

As already noted, $\xi_{\mathbf{k}}$ is defined by $\varepsilon_{\mathbf{k}} - E_F$. $\mathbf{k}$ is the wave number characterizing the CP, so that $\varepsilon_{\mathbf{k}}$ giving an electron energy should be evaluated for the crystal constructed from only SL because there are no CP's in the IL. In Sec. III, it is described how the band structure calculation is carried out for BSCCO consisting of periodic SL's.

## III. BAND-STRUCTURE CALCULATION

The SL in BSCCO consists of three atomic layers, lower-$CuO_2$, Ca, and upper-$CuO_2$ atomic layers, as shown in Fig. 2. The distance between the lower-$CuO_2$ and Ca atomic layers is the same as that between the Ca and upper-$CuO_2$ atomic layers, and the attractive interaction between the calcium atom and eight oxygen atoms (four oxygens are from the lower $CuO_2$ plane and the others the upper one) acts as a binding force to form the SL in BSCCO. Therefore, the interaction between the calcium and oxygen atoms must be taken into account in the band-structure calculation. In addition to the Ca-O interactions one should also consider the first-neighbor interactions of the Cu-O intra layer and the

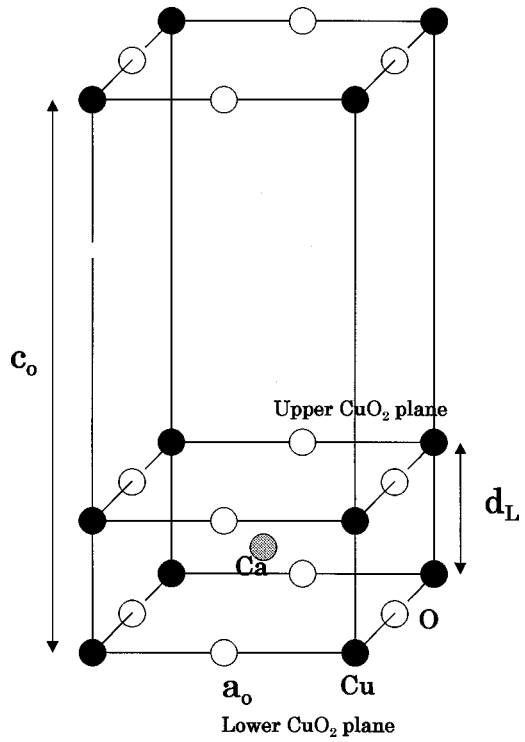


FIG. 2. Unit cell of a crystal consisting of only the periodic superconducting layers (SL's) extracted from $Bi_2Sr_2CaCu_2O_{8+\delta}$ (BSCCO).

Cu-Cu and O-O interlayers. This is done here by adopting the band-structure calculation based on the tight-binding (TB) method. In the TB method, generally, interactions between distant atoms such as second- and third- (and so on) nearest-neighbor atoms exist,[26] however it is possible to obtain the TB parameters optimized for only the dominant interactions which are usually the first-nearest-neighbor interactions. Harrison proposed optimal parameters called ''universal parameters'' which lead the fundamental interactions between atomic orbitals such as $sp\sigma$, $pp\sigma$, $pd\pi$ bonds, etc.[27] In the present paper, therefore, the band structure of the crystal consisting of periodic SL's is calculated by using the universal tight-binding parameters (UTBP) method.

In general, $3d$, $4s$, and $4p$ atomic orbitals of Cu, $\phi_{3d}^{(Cu)}$, $\phi_{4s}^{(Cu)}$ and $\phi_{4p}^{(Cu)}$, $2s$, and $2p$ ones orbitals of O, $\phi_{2s}^{(O)}$ and $\phi_{2p}^{(O)}$, and a $4s$ orbital Ca, $\phi_{4s}^{(Ca)}$ should be adopted as the basis functions which comprise the Bloch states. However, we are now focussing our attention to the electronic states near the Fermi level. In this case, it is enough to use the atomic orbitals $\phi_{3d}^{(Cu)}$, $\phi_{2p}^{(O)}$, and $\phi_{4s}^{(Ca)}$ in the UTBP band structure calculation for BSCCO. The self-energies of these orbitals are calculated by using the self-consistent-field (SCF) atomic structure calculations based on the Herman and Skillman prescription[28] using the Schwarz exchange correlation parameters.[29]

The first Brillouin zone with the volume $\Omega$ used in the present band-structure calculation is shown in Fig. 3 together with the reduced zone surrounded by six special points $\Gamma$, *X*, *M*, *Z*, *R*, and *A* with the volume $\Omega'(=\Omega/16)$. From symmetry

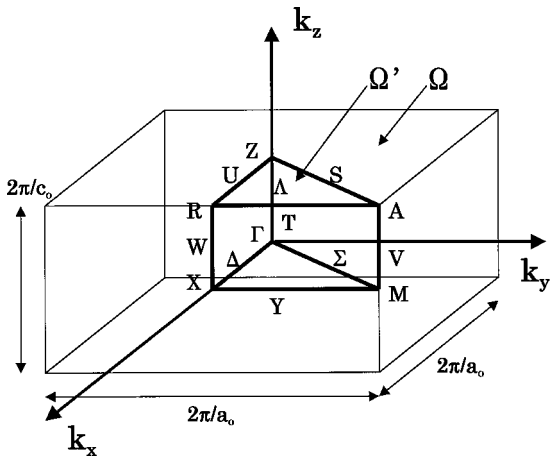


FIG. 3. The first Brillouin zone (BZ) used in the present band structure calculation. Six special points $\Gamma$, *X*, *M*, *Z*, *R*, and *A* and nine special lines $\Delta$, $\Sigma$, *Y*, *U*, *S*, *T*, $\Lambda$, *W*, and *V* are also shown.

considerations, the sum by $\mathbf{k}$ of an arbitrary function $F(\mathbf{k})$ having the $D_{4h}$ symmetry and the no electron-spin dependence, $\Sigma_{\mathbf{k}}^{\Omega} F(\mathbf{k})$, can be evaluated as $2\Sigma_{\mathbf{k}}^{\Omega'} g_{D_{4h}}(\mathbf{k}) F(\mathbf{k})$, where 2 is the degeneracy for the electron-spin and the $g_{D_{4h}}(\mathbf{k})$ is the number of stars of the wavenumver $\mathbf{k}$ tabulated in Table I. Therefore, the total density of states $N(E)$ and the partial density of states $D_L^{(\mu)}(E)$ for the $L$ orbital of $\mu$-atom are calculated as

$$N(E) = 2\sum_{\mathbf{k}}^{\Omega'} g_{D_{4h}}(\mathbf{k})\,\delta(E-\varepsilon_{\mathbf{k}}) \tag{21}$$

and

$$D_L^{(\mu)}(E) = 2\sum_{\mathbf{k}}^{\Omega'} |u_L^{(\mu)}(\mathbf{k})|^2 g_{D_{4h}}(\mathbf{k})\,\delta(E-\varepsilon_{\mathbf{k}}), \tag{22}$$

where $u_L^{(\mu)}(\mathbf{k})$ is the coefficient in the expansion of the total wave fuction $\Psi_{\mathbf{k}}(\mathbf{r})$ by the Bloch functions $\chi_L^{(\mu)}(\mathbf{k},\mathbf{r})$; that is, $\Psi_{\mathbf{k}}(\mathbf{r})$ is represented as

$$\Psi_{\mathbf{k}}(\mathbf{r}) = \sum_{\mu}\sum_{L} u_L^{(\mu)}(\mathbf{k})\chi_L^{(\mu)}(\mathbf{k},\mathbf{r}). \tag{23}$$

The calculations of the densities of states are carried out on the basis of the manner mentioned above, however, the sum $\Sigma_{\mathbf{k}(k_z>0)}$ in Eq. (11) must be done within the restricted area defined by $k_z>0$, so in this case the sum is evaluated as

TABLE I. The number of stars $g_{D_{4h}}(\mathbf{k})$ of the wave number $\mathbf{k}$ with $D_{4h}$ symmetry. Note that the value of $g_{D_{4h}}(\mathbf{k})$ is 16 for $\mathbf{k}$ within the reduced zone $\Omega'$ surrounded by six special points $\Gamma$, *X*, *M*, *Z*, *R*, and *A*, and is 8 for $\mathbf{k}$ on the five surfaces which comprise the reduced zone.

| $\mathbf{k}$ | $\Gamma,M,Z,A$ | $X,R$ | $\Delta,\Sigma,Y,U,S,T,W$ | $\Lambda,V$ |
|---|---|---|---|---|
| $g_{D_{4h}}(\mathbf{k})$ | 1 | 2 | 4 | 2 |

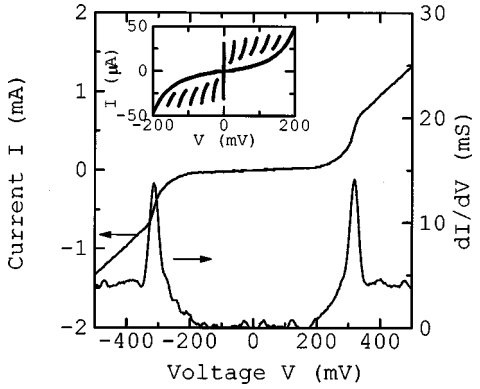


FIG. 4. Typical $I$-$V$ characteristics of a mesa with an area of 4 $\mu$m$^2$ at 4.2 K. The inset shows the $I$-$V$ characteristic in enlarged scale. This mesa contains six IJJ's. The differential conductivity $dI/dV$ is also shown as a function of $V$.

$$\sum_{\mathbf{k}(k_z>0)} F(\mathbf{k}) = \sum_{\mathbf{k}(k_z>0)}^{\Omega} F(\mathbf{k}) = 2 \sum_{\mathbf{k}(k_z>0)}^{\Omega'} \frac{g_{D_{4h}}(\mathbf{k})}{2} F(\mathbf{k}), \tag{24}$$

where we note that the fraction which appears in the final term is caused by the restricted sum defined by $k_z>0$.

## IV. EXPERIMENTS

### A. Samples and measurement

Measurements of the $I$-$V$ characteristics of IJJ's have been performed with mesa structures patterned on BSCCO single crystals. The BSCCO single crystals were grown by a self-flux technique, details of which were described elsewhere.[9] Their critical temperature $T_c$ were 80–85 K. In order to avoid the heating effect and to study inherent tunneling property in IJJ's, small mesas with area of 1, 4, and 25 $\mu$m$^2$ and with heights of 2–30 nm were fabricated on top of BSCCO single crystals using electron-beam lithography and Ar-ion milling.[30] The top contacts on the mesa and leads were provided by a gold film. The $I$-$V$ characteristics along the $c$ axis of the mesa were measured at liquid-helium temperature (4.2 K) by a three-terminal method. In a three-terminal configuration, the voltage comes from the mesa and the contact resistance between the measurements lead (Au) and BSCCO single crystal. For data evaluation below, therefore, the contact resistance has been subtracted.

### B. Tunneling property of IJJ's

The inset of Fig. 4 shows a typical $I$-$V$ characteristic at small current bias of a mesa with an area of 4 $\mu$m$^2$. The height of the mesa is about 10 nm, which is extrapolated from the etching rate. The $I$-$V$ characteristic exhibits multiple QP branches with large hysteresis due to the Josephson and quasiparticle tunneling. From the number of branches, one can easily estimate that this mesa consists of six IJJ's, which is in fairly good agreement with the expected one from the mesa height. Here it should be noted that the six QP branches do not show a negative resistance behavior. It is well known that such a behavior is observed in $I$-$V$ characteristics of mesas with large number of IJJ's,[24] and that it is attributed to the nonequilibrium effect. The model presented in this paper, however, does not include the nonequilibrium effect because it is hard to take into account it correctly. Moreover, in experiments it is difficult to distinguish equilibrium from nonequilibrium effects. For these reasons, the experimental data to be compared with our model must be obtained in equilibrium condition. To this purpose, we have selected a BSCCO sample with six IJJ's, where it is expected that the nonequilibrium effect is negligible.

The critical current $I_c$ of IJJ's in this mesa ranges from 30 to 38 $\mu$A, which corresponds to the critical current density $J_c$ of 750–950 A/cm$^2$. The characteristic voltage $V_c$, defined as the voltage jump at the critical current, was $\sim$32 mV. This value is much smaller than gap voltage $V_g = 2\Delta/e$ due to small $I_c$ and large leak current in contrast with a stack of conventional Josephson junctions made from BCS superconductors in which $V_c$ is equal or close to $V_g$. On a large current bias, a clear gap structure without negative resistance, confirming that interlayer transport occurs via tunneling process, appears as shown in Fig. 4. Moreover, the $I$-$V$ characteristic becomes linear at larger voltages, so that we can define the normal resistance $R_n$ of 61$\Omega$ per one junction for this mesa. From the $dI/dV-V$ curve shown in Fig. 4, the sum-gap voltage $NV_g$ was estimated to be 317 mV. As a result, we obtain an energy gap of $2\Delta = 53$ meV. Due to the improvement of the overheating problem by decreasing mesa area, this value is larger than that reported in early experiments[10,12] in IJJ's but is in good agreement with that obtained previously in surface tunneling experiments.[31] In addition, our experiments showed a good reproducibility. Therefore, we belive that the quasiparticle $I$-$V$ characteristic shown in Fig. 4 is a reflection of the inherent properties of IJJ's. From the experiments more than 30 mesas, we found that (1) the value of $2\Delta$ is 50–60 meV, and (2) their normalized quasiparticle $I$-$V$ characteristics have no sizable differences. Here the normalization has been done by $2N\Delta/e$ for the voltage and by $2\Delta/(eR_n)$ for the current, so that the normalized $I$-$V$ characteristic corresponds to that for a single junction.

The normalized $I$-$V$ characteristic of an IJJ is shown in Fig. 5(a), together with the calculated $I$-$V$ characteristics (b) and (c) by using traditional DOS model given by Eq. (1). Here note that the Fig. 5(b) was obtained by using the $\phi$-independent constant value as $N_n(\phi)$ defined in Eq. (2) and the Fig. 5(c) was obtained by using $\phi$-dependent $N_n(\phi)$ such as $1+\alpha\cos 4\phi$[31] with an adjustable parameter $\alpha=0.8$. Clearly, the experimental curve is found to be in good agreement with the curve Fig. 5(c) rather than the Fig. 5(b). This result suggests that the quasiparticle tunneling in IJJ's is much angle dependent rather than that in the simple $d$-wave DOS model. However, we must note that the above $\phi$-dependent $N_n(\phi)$ is a phenomenological expression. Thus for an exact analysis of our data we have to use the present model, which gives the quasiparticle tunneling current taking into accout the crystal symmetry.

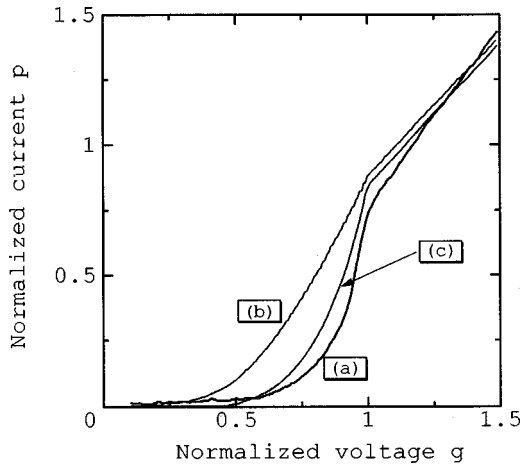


FIG. 5. Normalized $I$-$V$ characteristic along the $c$ axis of a $Bi_2Sr_2CaCu_2O_{8+\delta}$ (BSCCO) single crystal obtained from the $I$-$V$ characteristic measurement at liquid-helium temperature for the mesa with an area of 4 $\mu m^2$ (a). (b) and (c), calculated from a traditional DOS model, are also shown for the comparison, where (b) and (c) were obtained by using the $\phi$-independent and dependent $N_n(\phi)$'s.

## V. RESULTS AND DISCUSSION

### A. Electronic structures

The DOS (states/eV superconducting layer) calculated for a crystal consisting of periodic SL's extracted from the $Bi_2Sr_2CaCu_2O_{8+\delta}$ with $\delta=0$, i.e., no hole doping BSCCO, is shown in Fig. 6(a), together with the partial densities of states(PDOS's) (states/eV atom) for the Cu $3d$, O $2p$ and Ca $4s$ atomic orbitals drawn in Figs. 6(b), 6(c), and 6(d), respectively. On the present band structure calculations based on the UTBP method, values of 3.817, 15.3, and 3.4 Å were used as those of the lattice constants $a_0$ and $c_0$ and the interlayer distance $d_L$ between upper and lower $CuO_2$ layers,[32] and values of $-10.70$, $-11.28$, and $-4.68$ eV were used as those of the self-energies of $\phi_{3d}^{(Cu)}$, $\phi_{2p}^{(O)}$ and $\phi_{4s}^{(Ca)}$ atomic orbitals which were obtained from the SCF atomic structure calculations. Figure 6 shows that the DOS $N(E)$ consists of a valence band located below circa $-7.5$ eV and a conduction band located around $-2.5$ eV, and that the valence band is mainly constructed from $\phi_{3d}^{(Cu)}$ and $\phi_{2p}^{(O)}$ atomic orbitals and almost all the conduction band is made from $\phi_{4s}^{(Ca)}$ one.

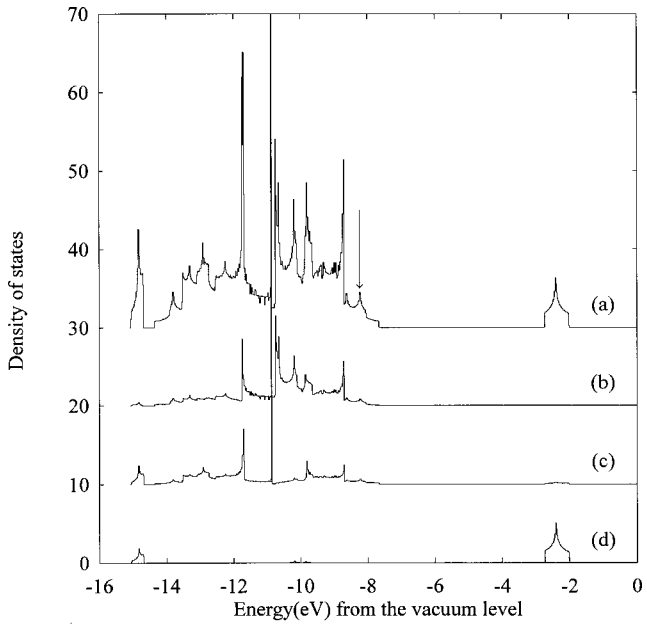


FIG. 6. Density of states (DOS) (states/eV superconducting layer) (a) and partial densities of states (PDOS's) (states/eV atom) calculated for (b) Cu $3d$, (c) O $2p$, and (d) Ca $4s$ atomic orbitals. The arrow drawn in (a) shows the energy position of the Fermi level $E_F$.

The BCS theory tells us that $T_c$ is correlated with the density of states at the Fermi level, $N(E_F)$, as follows:

$$k_B T_c = 1.14\hbar\omega_D e^{-1/V_0 N(E_F)}. \tag{25}$$

It is not correct to apply all the predictions deduced from the BCS theory into the high-$T_c$ superconductor, but it could not be wrong to suppose that the highest critical temperature is obtained when the $N(E_F)$ has the largest value. In the present paper, therefore, we adopt the energy position indicated by an arrow in Fig. 6 as the Fermi level $E_F$, in which $N(E_F)$ has the maximum value. The justification to use this energy position as the $E_F$ is presented as follows; On the $Bi_2Sr_2CaCu_2O_{8+\delta}$ (BSCCO), it is well known that the hole doping plays an essential role to genarate the superconducting state and that the superconducting state of the BSCOO with $T_c \sim 90(K)$ appears when the value of $\delta$ is around 0.24 (/unit cell).[33] The value of $\delta$ characterizes the amount of oxygen dopant into the $Bi_2Sr_2CaCu_2O_8$ unit cell. If a SL captures the doped oxygens, this process makes the change of symmetry of the SL. Then, it could be natural to suppose that the IL rather than the SL accepts the doped oxygens. If the $\delta$ numbers of oxygen are captured by the IL, $2\delta$ electrons must transfer from the SL to the IL because the oxygen in the IL should be ionized as $O^{-2}$. This charge transfer leads the change of the ionicity of oxygens in the SL. There are four oxygens (/unit cell) in the SL, so that the respective oxygen must release $2\delta/4$ electrons on the charge transfer process. That is, if we denote the ionicity of oxygen in the SL as $-q(q>0)$, i.e., $O^{-q}$, we can see that a relation

$$q = 2 - \frac{\delta}{2}, \tag{26}$$

is deduced between $\delta$ and $q$, and that $q$ must be given so as to satisfy the following relation;

$$\int_{-\infty}^{E_F} D_{2p}^{(O)}(E)dE = 4 + q, \tag{27}$$

where $D_{2p}^{(O)}(E)$ is the partial density of states (PDOS) (states/eV atom) for the oxygen $2p$ orbital in the SL. The PDOS is the projected value of the total density of states into an orbital to be considered, so, exactly speaking, $D_{2p}^{(O)}(E)$ must be deduced from the band-structure calculations including not only SL's but also IL's. We are now interested in the value of $\xi_{\mathbf{k}}$ as a function of the wave number $\mathbf{k}$ characteriz-

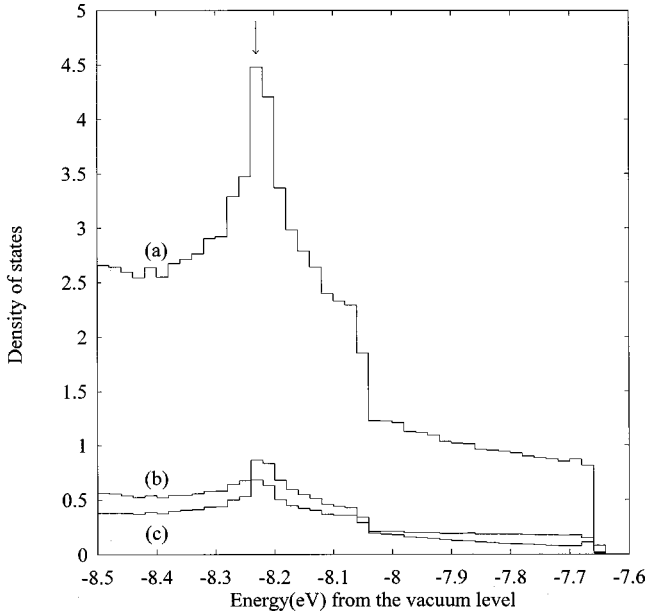


FIG. 7. Density of states (DOS) (states/eV superconducting layer) (a) and partial densities of states (PDOS's) (states/eV atom) of (b) Cu $3d$ and (c) O $2p$ orbitals near the Fermi level $E_F$ indicated by an arrow in (a).

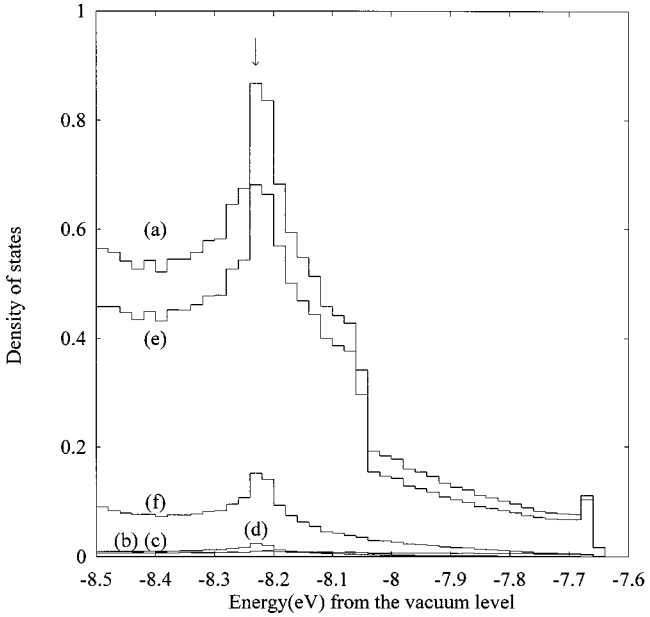


FIG. 8. Partial densities of states (PDOS's) (states/eV atom) for (a) $3d$, (b) $3d_{xy}$, (c) $3d_{yz}$, (d) $3d_{zx}$, (e) $3d_{x^2-y^2}$, and (f) $3d_{3z^2-r^2}$ orbitals of a Cu atom near the Fermi level $E_F$ indicated by an arrow.

ing a CP, so that the band-structure calculations carried out in the present paper do not include the IL's. Therefore, the value of $q$ evaluated from Eq. (27) could somewhat differ from the value of $\sim 1.88$ with $\delta \sim 0.24$. The value of $q$ calculated by using $E_F$ represented in Fig. 6 was 1.845.

We are now interested in the electronic states near $E_F$ consisting of the Cu $3d$ and O $2p$ atomic orbitals. $N(E)$, $D_{3d}^{(Cu)}(E)$, and $D_{2p}^{(O)}(E)$ near $E_F$ are shown in Figs. 7(a), 7(b) and 7(c), and in order to see the nature of the $D_{3d}^{(Cu)}(E)$ and $D_{2p}^{(O)}(E)$ more explicitly, $D_{3d}^{(Cu)}(E)$, $D_{3d_{xy}}^{(Cu)}(E)$, $D_{3d_{yz}}^{(Cu)}(E)$, $D_{3d_{zx}}^{(Cu)}(E)$, $D_{3d_{x^2-y^2}}^{(Cu)}(E)$ and $D_{3d_{3z^2-r^2}}^{(Cu)}(E)$ are shown in Figs. 8(a), 8(b), 8(c), 8(d), 8(e) and 8(f), and $D_{2p}^{(O)}(E)$, $D_{2p_x}^{(O)}(E)$, $D_{2p_y}^{(O)}(E)$, and $D_{2p_z}^{(O)}(E)$ are shown in Figs. 9(a), 9(b), 9(c), and 9(d). Here we note that the oxygen adopted in Fig. 9 makes a Cu-O-Cu chain along the $y$ direction, so that $D_{2p_x}^{(O)}(E)$ and $D_{2p_y}^{(O)}(E)$ must replace each other when the oxygen in the Cu-O-Cu chain oriented to the $x$ direction is adopted. Figures 8 and 9 show that $D_{3d}^{(Cu)}(E)$ is mainly constructed from the Cu $3d_{x^2-y^2}$ orbital and $D_{2p}^{(O)}(E)$ is made from the $2p_\sigma$ one, where the $2p_\sigma$ orbital is a $2p_{x(y)}$ orbital of oxygen in the Cu-O-Cu chain oriented in the $x(y)$ direction. Therefore, we conclude that almost all electronic states near the Fermi level are made by the $pd\sigma$-state caused by Cu $3d_{x^2-y^2}$ and O $2p_\sigma$ atomic orbitals.

### B. QP $I$-$V$ characteristic

In this section, we present the calculated results of the QP $I$-$V$ characteristic and compare those with the experimental results. First we present the results obtained by using the energy gap $\Delta_{\mathbf{k}}$ with $n=0$, i.e., a purely two-dimensional $\cos 2\phi$-type enegy gap. Next we present those with $n \neq 0$ in order to see how the change of the dimensionality of the energy gap influences into the QP $I$-$V$ characteristic. In all the calculations presented in this section, the values of 53 meV and 4.2 K were used as those of $2|\Delta(T)|[\equiv eV_m(T)]$ and the sample temperature $T$.

#### *1. Case of $\Delta_{\mathbf{k}}$ with $n=0$*

The normalized QP $I$-$V$ characteristic with $n=0$, calculated by using the values of $\xi_{\mathbf{k}}$ obtained from the band-

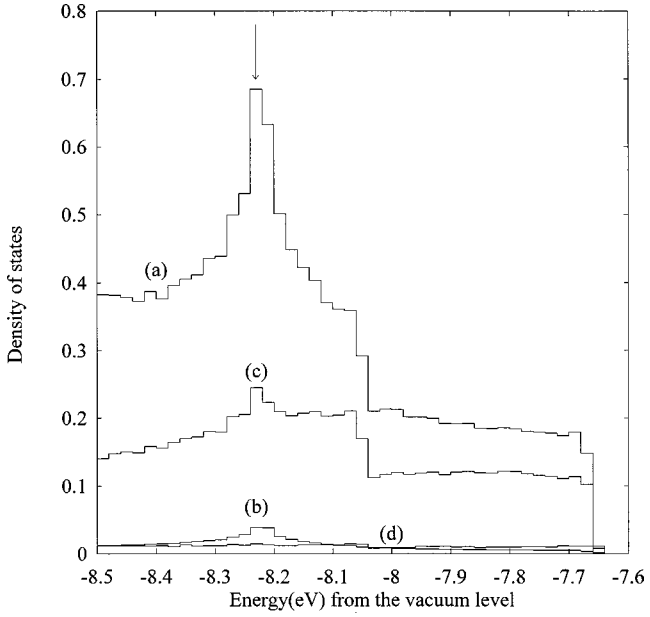


FIG. 9. Partial densities of states (PDOS's) (states/eV atom) for (a) $2p$, (b) $2p_x$, (c) $2p_y$, and (d) $2p_z$ orbitals of an O atom near the Fermi level $E_F$ indicated by an arrow. Note that the oxygen adopted here is an oxygen in the Cu-O-Cu chain oriented in the $y$ direction.

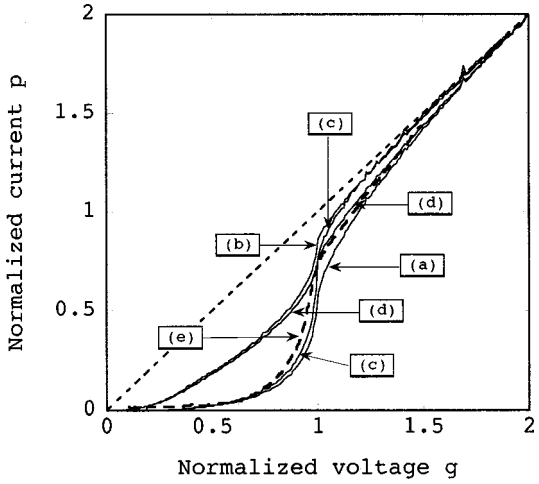


FIG. 10. Normalized quasiparticle (QP) tunneling current-voltage ($I$-$V$) characteristics calculated under the conditions of (a) **k**-dependent weight $w_{\mathbf{k}}$ and charge $q_{\mathbf{k}}$ denoted as $(w_{\mathbf{k}},q_{\mathbf{k}})$, (b) **k**-independent weight and charge denoted as $(1,q)$, (c) **k**-independent weight and **k**-dependent charge $q_{\mathbf{k}}$ $(1,q_{\mathbf{k}})$ and (d) **k**-dependent weight $w_{\mathbf{k}}$ and **k**-independent charge $(w_{\mathbf{k}},q)$. Curve (e) is an experimental $I$-$V$ characteristic to be compared with the calculated ones. Note that the normalized voltage $g$ and current $p$ have been defined as $V/V_m$ and $2I(g)/I(g=2)$, where $eV_m \equiv 2|\Delta(T)|$.

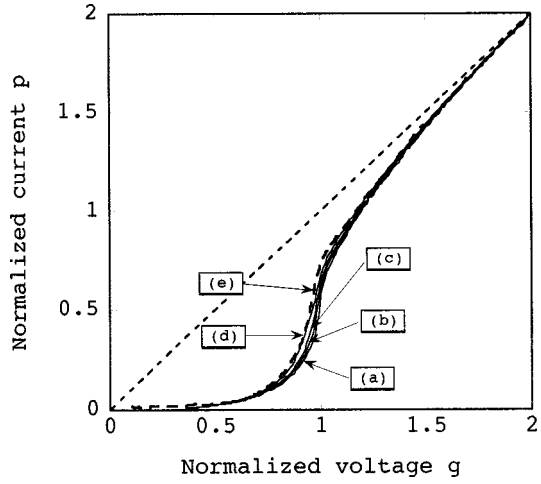


FIG. 11. Normalized quasiparticle (QP) tunneling current-voltage ($I$-$V$) characteristics calculated under the conditions of **k**-dependent weight and charge $(w_{\mathbf{k}},q_{\mathbf{k}})$ and (a) $n=0$, (b) $n=0.5$, (c) $n=1$, and (d) $n=2$. Curve (e) is a normalized experimental $I$-$V$ characteristic. Note that $n$ is the value characterizing the dimensionality of the energy gap $\Delta_{\mathbf{k}}$ defined in Eq. (19).

structure calculation, is shown in Fig. 10(a). Here the normalization has been done so that the voltage $V$ is represented by the normalized voltage $g(T)$ defined by $V/V_m(T)$ and the normalized current $p$ calculated on the normalized voltage with the value of 2 is equal to 2. In addition to a curve shown in Fig. 10(a) calculated under the condition of **k**-dependent weight $w(-\lambda_{\mathbf{k}},\Delta_{\mathbf{k}})$ defined by Eq. (7) and charge $q_{\mathbf{k}}$ defined by Eq. (20) denoted as $(w_{\mathbf{k}},q_{\mathbf{k}})$, the curves calculated under the conditions of $(1,q)$, $(1,q_{\mathbf{k}})$ and $(w_{\mathbf{k}},q)$ are shown in Figs. 10(b), 10(c), and 10(d), respectively, together with the experimental $I$-$V$ characteristic shown in Fig. 10(e). Here note that a curve shown in Fig. 10(b) calculated by our model corresponds to the $I$-$V$ characteristic shown in Fig. 5(b) calculated by using a traditional DOS model. The reason why the curve (b) in Fig. 10 and the curve (b) in Fig. 5 do not coincide with each other perfectly could be caused by the fact that the DOS model cannot take into account the symmetry of the crystal and the energy gap correctly because of the integral by $E$, as already stated. Figure 10 clearly shows that curves (b) and (d) in which a **k**-independent QP charge has been adopted, are far from the experimental curve (e). Both the curves (a) and (c) using the $q_{\mathbf{k}}$ seem to predict the experimental curve (e) fairly well. However it is found that the deviation at the high voltage region $(g>1)$ of the curve (c) using the **k**-independent weight from the experiment is larger than that of the curve (a) using the **k**-dependent weight $w_{\mathbf{k}}$. Therefore, we can conclude that the QP $I$-$V$ characteristic calculated under the condition of $(w_{\mathbf{k}},q_{\mathbf{k}})$ gives the best result. Figure 10 shows that the curve (a) underestimates the experimental curve (e). This point will be clarified in the next subsection.

### *2. Case of $\Delta_{\mathbf{k}}$ with $n\neq 0$*

Here we consider the effect of the dimensionality of the energy gap into the QP $I$-$V$ characteristic. The condition $(w_{\mathbf{k}},q_{\mathbf{k}})$ gives the best result, so that all the calculations presented here are carried out under the condition of **k**-dependent weight and charge.

We have tentatively selected the values of 0.5, 1, and 2 as those of $n$. The normalized QP $I$-$V$ characteristics calculated under the conditions of $n=0$, 0.5, 1 and 2 are shown in Figs. 11(a), 11(b), 11(c), and 11(d) together with the experimental curve shown in Fig. 11(e). The effect of $n$ is not so large, but appears arround the normalized voltage $g\sim 1$. The effect due to the increasing of $n$ is that the gradient $dp/dg$ arround $g=1$ of the normalized current $p(\equiv 2I(g)/I(g=2))$ decreases and the calculated QP $I$-$V$ characteristic gradually reaches the experiment. From Fig. 11, we can see that curve (d) using $n=2$ is in very good agreement with our experimental curve (e). Therefore, if we take into account the experimental errors, it may be reasonable to suppose that the angular dependence of the energy gap $\Delta_{\mathbf{k}}$ should be given as $(\theta,\phi)$ dependent such as $\sin^{2n}\theta\cos 2\phi$ with $n\sim 2$ rather than the $\theta$-independent purely two dimensional $\cos 2\phi$-type.

## VI. SUMMARY

We have proposed a model to understand the overall profile of QP $I$-$V$ characteristic of intrinsic Josephson junctions in BSCCO. Using the values of $\xi_{\mathbf{k}}$ obtained from band structure calculations based on the universal tight-binding parameters method, the QP $I$-$V$ characteristics have been calculated with no adjustable parameters. It has been pointed out that the angular dependence of the energy gap $\Delta_{\mathbf{k}}$ of the high-$T_c$ superconductors such as $Bi_2Sr_2CaCu_2O_{8+\delta}$ should be represented as being of $\sin^{2n}\theta\cos 2\phi$ type rather than of $\theta$-independent purely two dimensional $\cos 2\phi$ type. From the fact that the QP's are generated by the separation of a CP

($\mathbf{k}\sigma,-\mathbf{k}\sigma'$), we have proposed that the charge of the QP ought to show the angular dependence such as $|\Delta_{\mathbf{k}}|^2$. From a comparison of the calculated results with the experimental ones, we have found that (1) the calculations are greatly improved by introducing the **k**-dependent QP charge $q_{\mathbf{k}}$, (2) the overall profile of the experimental *I-V* characteristic is fairly well explained by including not only the $q_{\mathbf{k}}$ but also the **k**-dependent weight $w(-\lambda_{\mathbf{k}},\Delta_{\mathbf{k}})$ which is the existing probability of the CP identified by the energy of $-\lambda_{\mathbf{k}}$; and (3) the QP *I-V* characteristic, calculated by using the energy gap $\Delta_{\mathbf{k}}$ with $n=2$, i.e., $\Delta(T)\sin^4\theta\cos 2\phi$, excellently reproduces the experimental *I-V* characteristic in whole voltage region. We wish to emphasize that the energy gap $\Delta_{\mathbf{k}}$ of the high-$T_c$ superconductors which is the most important quantity on the study of the superconductors ought to show not only the $\phi$ dependence but also the $\theta$ dependence.


[1] J.G. Bednorz and K.A. Müller, Z. Phys. B: Condens. Matter **64**, 189 (1986).
[2] M.K. Wu, J.R. Ashburn, C.J. Huang, Y.Q. Wang, and C.W. Chu, Phys. Rev. Lett. **58**, 908 (1987).
[3] H. Maeda, Y. Tanaka, M. Fukutomi, and T. Asano, Jpn. J. Appl. Phys. **27**, L209 (1988).
[4] Z.Z. Sheng and A.M. Hermann, Nature (London) **232**, 55 (1988).
[5] A. Schilling, M. Cantoni, J.D. Guo, and H.R. Ott, Nature (London) **363**, 56 (1993).
[6] R. Kleiner, F. Steinmeyer, G. Kunkel, and P. Müller, Phys. Rev. Lett. **68**, 2394 (1992).
[7] R. Kleiner and P. Müller, Phys. Rev. B **49**, 1327 (1994).
[8] G. Oya, N. Aoyama, A. Irie, S. Kishida, and H. Tokutaka, Jpn. J. Appl. Phys. **31**, L829 (1992).
[9] A. Irie, M. Sakakibara, and G. Oya, IEICE Trans. Electron. **E77-C**, 1191 (1994).
[10] A. Yurgens, D. Winkler, N.V. Zavaritsky, and T. Claeson, Phys. Rev. B **53**, R8887 (1996).
[11] Yu.I. Latyshev, J.E. Nevelskaya, and P. Monceau, Phys. Rev. Lett. **77**, 932 (1996).
[12] K. Tanabe, Y. Hidaka, S. Karimoto, and M. Suzuki, Phys. Rev. B **53**, 9348 (1996).
[13] M. Rapp, A. Murk, R. Semerad, and W. Prusseit, Phys. Rev. Lett. **77**, 928 (1996).
[14] M. Itoh, S. Karimoto, K. Namekawa, and M. Suzuki, Phys. Rev. B **55**, 12001 (1997).
[15] A. Irie, T. Mimura, M. Okano, and G. Oya, Supercond. Sci. Technol. **14**, 1097 (2001).
[16] M. Tinkham, *Introduction to Superconductivity* 2nd ed. (McGraw-Hill, New York, 1996).
[17] A. Barone and G. Paterno, *Physics and Applications of the Josephson Effect* (Wiley, New York, 1982).
[18] D.A. Wollman, D.J. van Harlingen, W.C. Lee, D.M. Ginsberg, and A.J. Leggett, Phys. Rev. Lett. **71**, 2134 (1993).
[19] T.P. Devereaux, D. Einzel, B. Stadlober, R. Hackl, D.H. Leach, and J.J. Neumeier, Phys. Rev. Lett. **72**, 396 (1994).
[20] C.C. Tsuei, J.R. Kirley, C.C. Chi, L.S. Yu-Jahnes, A. Gupta, T. Shaw, J.Z. Sun, and M.B. Ketchen, Phys. Rev. Lett. **73**, 593 (1994).
[21] D.J. van Harlingen, Rev. Mod. Phys. **67**, 515 (1995).
[22] O. Waldman, F. Steinmeyer, P. Müller, J.J. Neumeier, F.X. Régi, H. Savary, and J. Schneck, Phys. Rev. B **53**, 11825 (1996).
[23] C.C. Tsuei and J.R. Kirtley, Rev. Mod. Phys. **72**, 969 (2000).
[24] K. Schlenga, R. Kleiner, G. Hechtfischer, M. Mößle, S. Schmitt, P. Müller, Ch. Helm, Ch. Preis, F. Forsthofer, J. Keller, H.L. Johnson, M. Veith, and E. Steinbeiß, Phys. Rev. B **57**, 14518 (1998).
[25] P. G. DE Gennes translated by P. A. Pincus, *Superconductivity of Metals and Alloys* (Benjamin, New York, 1966).
[26] M. Kitamura and S. Muramatsu, Phys. Rev. B **41**, 1158 (1990).
[27] W. A. Harrison, *Elementary Electronic Structure* (World Scientific, Singapore, 1999).
[28] F. Herman and S. Skillman, *Atomic Structure Calculations* (Prentice-Hall, Englewood Cliffs, NJ, 1963).
[29] K. Schwarz, Phys. Rev. B **5**, 2466 (1972).
[30] A. Irie, G. Oya, R. Kleiner, and P. Müller, Physica C **362**, 145 (2001).
[31] C. Manabe, M. Oda, and M. Ido, J. Phys. Soc. Jpn. **66**, 1776 (1997).
[32] J.M. Tarascon, Y. LePage, P. Barboux, B.G. Bagley, L.H. Greene, W.R. McKinnon, G.W. Hull, M. Giroud, and D.M. Hwang, Phys. Rev. B **37**, 9382 (1988).
[33] T. Watanabe, T. Fujii, and A. Matsuda, Phys. Rev. Lett. **79**, 2113 (1997).